Dynamic Phenomena in Self-Complementary {2}-Metallocryptates Probed by Solution ^{133}Cs-NMR. New Insights into Ion Pairing Processes: X-Ray Structure and Solid-State NMR Spectra of a Meandering Species

by **Harald Maid**[a]), **Frank W. Heinemann**[b]), **Andreas Scheurer**[b]), **Nicolai Mooren**[a]), **Rolf W. Saalfrank**[b]), and **Walter Bauer***[a])

[a]) Department Chemie und Pharmazie, Lehrstuhl für Organische Chemie II, Friedrich-Alexander-Universität Erlangen-Nürnberg, Henkestrasse 42, D-91054 Erlangen (phone: +49-9131-8522991; fax: +49-9131-8522991; e-mail: bauer@chemie.uni-erlangen.de)

[b]) Department Chemie und Pharmazie, Lehrstuhl für Anorganische und Allgemeine Chemie, Friedrich-Alexander-Universität Erlangen-Nürnberg, Egerlandstrasse 1, D-91058 Erlangen

Dedicated to Prof. Dr. Dr. h.c. *Dieter Seebach* on the occasion of his 75th birthday

Two self-complementary {2}-metallocryptates, differing in methyl and phenyl substituents, respectively, have been studied by X-ray analysis, and solid-state and solution NMR. Mixed Mg/Cs metal methyl complex **2** is a linear polymer in the solid state. The two different Cs sites are confirmed by ^{133}Cs-solid-state NMR. By contrast, the analog mixed Mg/Cs metal phenyl complex **4** is a meandering polymer as shown by an actual X-ray analysis. The four non-equivalent Cs-sites in **4** are reflected in the solid-state NMR spectra. Solution ^{133}Cs-NMR spectra of **4** reveal two independent dynamic processes: a fast exchange of Cs within contact ion-pairs and solvent-separated ion-pairs (CIP, SSIP), and a slower exchange of 'inside' *endo* Cs, surrounded by three ligands, and 'outside' *exo* Cs involved in the CIP/SSIP equilibrium. Complete line-shape analysis of variable-temperature ^{133}Cs-NMR spectra of **4** yield kinetic parameters of $\Delta G^{\ddagger}_{253} = 10.8$ kcal/mol for the fast SSIP-CIP exchange and $\Delta G^{\ddagger}_{308} = 13.2$ kcal/mol for the slower *endo*/*exo* exchange of Cs. DOSY-NMR Measurements confirm the monomeric nature of **4** in solution.

Introduction. – By complexation of Mg^{II} ions in the presence of Cs ions, catechole derived bis-diketone **1** forms a racemic mixture of homochiral metallocryptate **2** (*Scheme 1*). The single negative charge of the complex is compensated by a Cs counter ion. In the solid state, this counter ion is arranged in an 'end-on' fashion. These self-complementary building blocks aggregate in the crystal and form a racemic arrangement of homochiral strands [1].

Under the same reaction conditions, metallocryptate **4** is formed from Ph-substituted ligand **3** (*Scheme 2*). For the analog, structurally characterized $[Cs \subset \{Co_2(L^2)_3\}]Cs$ and $[Rb \subset \{Mg_2(L^2)_3\}]Rb$, and in contrast to **2**, a meandering coordination polymer is formed in the crystal [1]. Here, two monomers of different chirality are linked by Cs or Rb, respectively, in an 'end-on' fashion. These *meso*-dimers, in turn, are linked by Cs or Rb, now in a 'side-on' fashion to form a *meso*-polymer.

Interactions between Cs ions and cryptands were and still are extensively studied. ^{133}Cs-NMR has been established as a valuable tool for determining the kinetic and thermodynamic parameters of a complexation [2]. However, already in 1977 *Popov*

Scheme 1. *Synthesis and Schematic Presentation of the Repeating Units of the Homochiral Strings* Δ-(**2**)$_n$ *and* Λ-(**2**)$_n$ (= *rac*-(**2**)$_n$) (top). *A Section from the Crystal Structure of* rac-(**2**)$_n$ *Showing the Δ Enantiomer* (bottom). Mg, dark grey; Cs, transparent light grey.

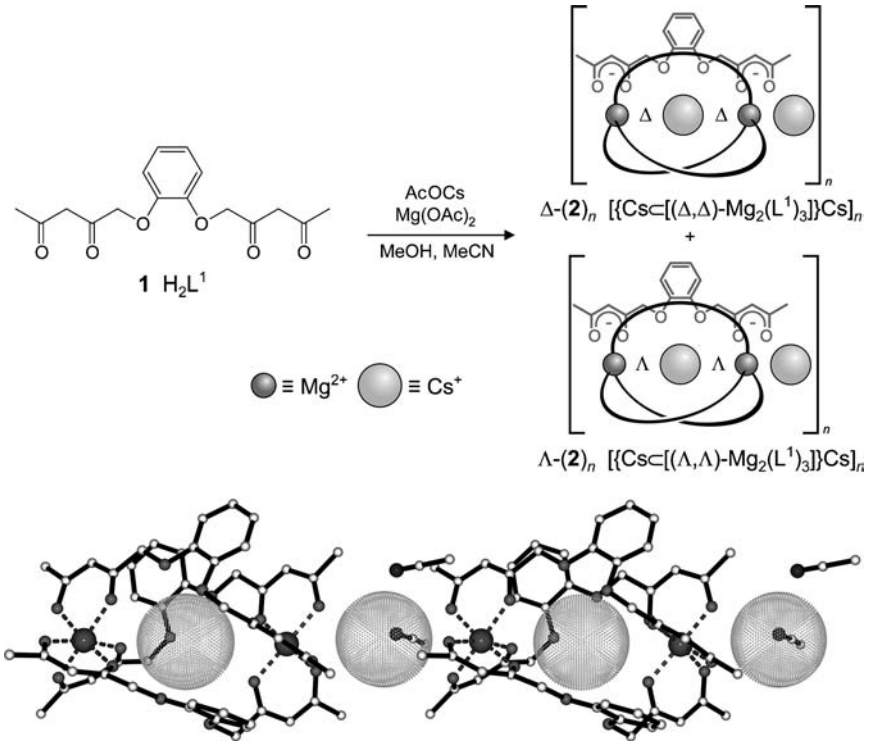

and co-workers showed that, in solution, Cs can form two types of complexes with cryptands [3]. Along with the classical cryptate, there is also an 'exclusive' cryptate in which the Cs-ion is only partially enclosed in the cavity of the ligand. Along with metallocryptates **2** and **4**, we here have the rare case that a stoichiometric compound features an *endo*- as well as an *exo*-Cs [4][5]. Since these metallocryptate monomers remain intact in solution and are stable with respect to a possible exchange of the Mg^{2+} centers, they are suitable for studying possible dynamics between *exo*- and *endo*-Cs. In this article, we explore *rac*-(**2**)$_n$ and *meso*-(**4**)$_n$ in the solid state as well as in solution by means of ^{133}Cs-NMR.

Results and Discussion. – For reasons of consistency and of a more intuitive approach to the contents of this article, we first describe the results obtained for complex **4**, followed by the description of complex **2**.

Phenyl Complex **4**. The recently carried out X-ray structure analysis of **4** revealed a meandering polymeric connectivity of Cs embedded within a cage of each three ligands ('*endo*-Cs') and 'outside' Cs ('*exo*'). The geometrical arrangement within the crystal is depicted in *Fig. 1* and is largely similar to the arrangement shown in *Scheme 2* for the analogous Co and Rb complexes. In **4**, there are pairs of homochiral entities ((Δ,Δ)$_2$

Scheme 2. *Synthesis of* **4** *together with a Schematic Presentation of the Proposed Arrangement in the Crystal by Analogy to the Structurally Characterized Co–Cs and Mg–Rb Complexes Described in the Text*

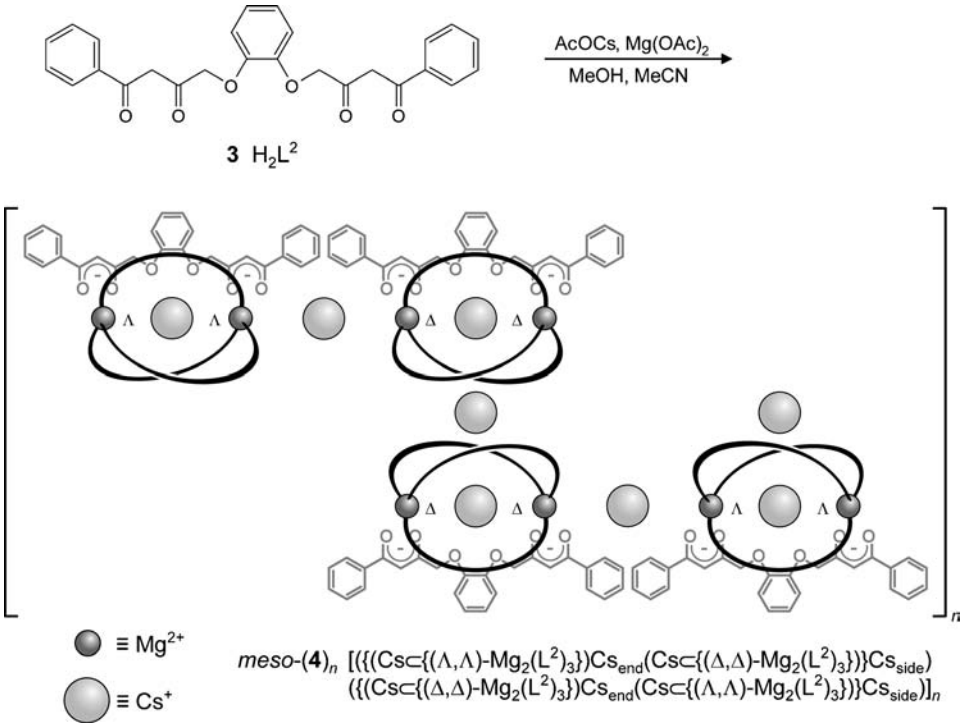

and $(\Lambda,\Lambda)_2$), each pair being linked by a 'side-on' Cs. However, these homochiral units (*e.g.*, (Δ,Δ)-(Δ,Δ)) have different conformations. Hence, there are four non-equivalent Cs sites in the unit cell of **4**.

Fig. 2 shows a stereoscopic view of two consecutive units of the unit cell and reflects the meandering nature within one 'strand'.

The solid-state ^{133}Cs-NMR spectrum of **4** was consistent with the situation found in the X-ray analysis: clearly, four distinct signals were found in the ^{133}Cs spectrum of **4** (*Fig. 3*). Partly by analogy to the solution-state spectrum (see below), we assigned the four signals as follows: δ 44.3 ppm, *endo*-Cs in $(\Delta,\Delta)^1$ or $(\Delta,\Delta)^2$ and their Λ-analogs; 41.1 ppm, *endo* Cs in $(\Delta,\Delta)^2$ or $(\Delta,\Delta)^1$ and their Λ-analogs; 13.8 ppm, *exo*-Cs, 'side-on' or 'end-on'; -22.7 ppm, *exo*-Cs, 'end-on' or 'side-on'.

Experimentally, the solid-state ^{133}Cs-NMR spectra of **4** had to be recorded quite quickly: outside the mother liquor and inside the MAS rotor, the powdered crystals decompose within *ca.* 30 min. due to loss of co-crystallized solvent (Et_2O, MeCN). The above assignment was confirmed by the finding that, with continuing decomposition of the material the low-field ^{133}Cs signals remained unaffected, whereas the high-field signals exhibited further splitting.

Solution ^{1}H- and ^{13}C-NMR spectra of **4** have been reported in [1]. The solution-state NMR spectra of **4** indicate that the polymeric nature of the crystal is not

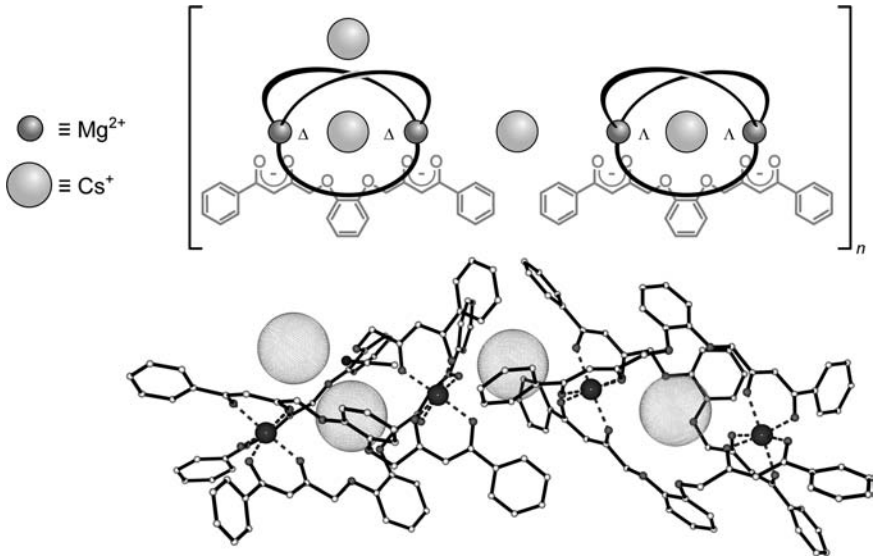

Fig. 1. *X-Ray structure of* meso-(**4**)$_n$. *Top:* schematic representation of the meandering asymmetric unit. *Bottom:* view of the asymmetric unit as detected by structural analysis. Co-crystallized solvent molecules (Et_2O, MeCN) have been omitted for clarity. Mg, dark grey, small; Cs, light grey, large.

maintained in (D_6)acetone: sharp signals were found in the ^{1}H- and ^{13}C-NMR spectra at room temperature, as expected for monomeric entities. However, when the ^{13}C-NMR spectrum of **4** was processed by the application of strong resolution enhancement (*Gauss* window), most but not all signals showed an additional splitting. Exemplarily, this is shown for the signals of the two C=O groups of the ligand within **4** in *Fig. 4*.

This splitting is compatible either with diastereotopic sites within a monomeric unit, or with the presence of two diastereoisomers. Since the signal intensities within the splitted pairs are slightly different, we prefer the latter explanation. Hence, we obviously observed at room temperature at the same time the racemate ($\Delta,\Delta/\Lambda,\Lambda$) as well as the *meso* compound (Δ,Λ) in slightly different concentrations [6]. From the very small ^{13}C-chemical shift differences of only *ca.* 0.04 ppm in *Fig. 4* (*ca.* 5 Hz at 11.7 T), we concluded that the exchange rate between the racemate and the *meso*-form must be quite small at room temperature[1]). In the case of **4**, ^{1}H-NMR spectra unfortunately were of no help in further confirming the co-existence of the racemate and the *meso*-form: for the potentially indicative OCH_2 H-atoms, only a broadened signal was observed [8].

The solution ^{133}Cs-NMR spectrum of **4** is depicted in *Fig. 5*. At first glance, there appear to be similarities to the solid-state NMR spectrum of *Fig. 3*. However, this similarity is partly accidental and must be attributed to ion-pair effects described below.

---

[1]) There are further examples presented by our group where 'stable' chiral conformations within tetranuclear complexes could be detected by NMR spectroscopy at room temperature [7].

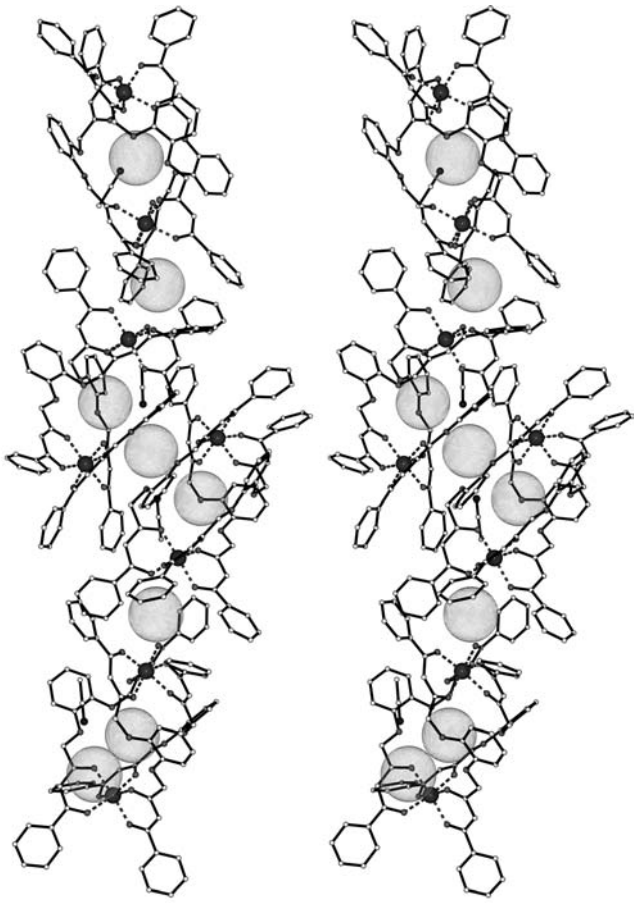

meso-(**4**)$_n$ [({(Cs⊂{(Λ,Λ)-$Mg_2(L^2)_3$})Cs_{end}(Cs⊂{(Δ,Δ)-$Mg_2(L^2)_3$})}Cs_{side})
({(Cs⊂{(Δ,Δ)-$Mg_2(L^2)_3$})Cs_{end}(Cs⊂{(Λ,Λ)-$Mg_2(L^2)_3$})}Cs_{side})]$_n$

Fig. 2. *Stereoscopic representation of two consecutive units of the unit cell of* **4**

We were intrigued by strong dynamic phenomena observed in the solution ^{133}Cs-NMR spectra at various temperatures. Thus, a series of temperature-dependent ^{133}Cs-NMR spectra was recorded. The experimental spectra, along with the corresponding simulations (complete line-shape analysis), are shown in *Fig. 6*.

^{133}Cs-VT-NMR Spectra of **4** were recorded in (D_6)acetone between $-80°$ and $+50°$ in $10°$ intervals[2]). At low temperatures, four signals were observed, with the signal at lowest field being present as a shoulder of the signal at slightly higher field

[2]) For the spectra simulations, the concentrations of the involved species (CIP and SSIP) were extrapolated from the integrals of the spectra at low temperatures, see *Supporting Information* (http://www.chemie.uni-erlangen.de/oc/bauer/SI/H12494-SI.pdf). Starting at $-80°$, the concentration of the CIP (contact ion pairs) increases with higher temperatures. Hence, the CIP → SSIP (solvent-separated ion pairs) reaction is an exothermic process.

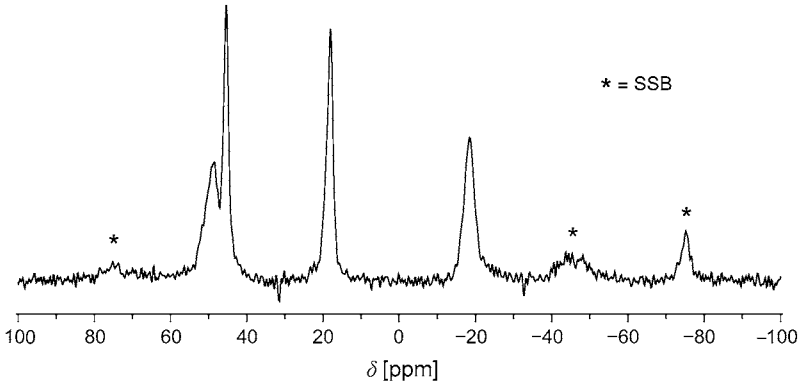

Fig. 3. *^{133}Cs{^{1}H}-Solid-state MAS-NMR spectrum of* **4**, *zoomed center region, recorded 15 min after rotor fill.* Measuring time, 9 min, spinning speed, 6117 Hz. Spinning side bands are marked by an asterisk. The four distinct signals reflect the four non-equivalent Cs sites present in the crystal unit cell.

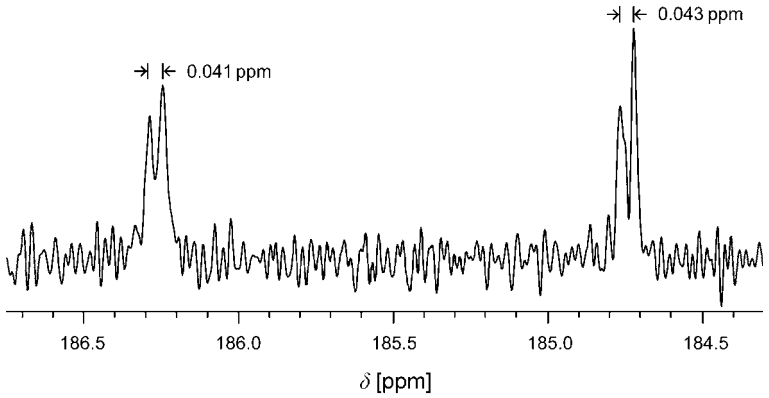

Fig. 4. *^{13}C-NMR Spectrum of* **4**, *zoomed region of C=O signals with strong resolution enhancement* (*Gauss* window) ((D$_6$)acetone, room temperature, measuring time, 75 h)

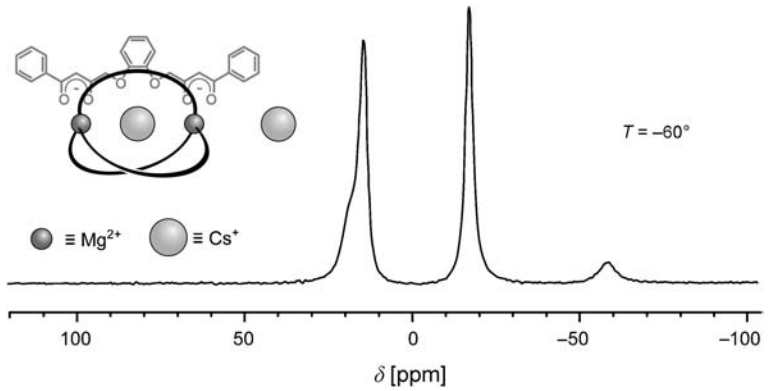

Fig. 5. *Solution ^{133}Cs{^{1}H}-NMR spectrum of* **4** *in (D$_6$)acetone at* $-60°$. The signal at lowest field is present as a shoulder in the signal at slightly higher field.

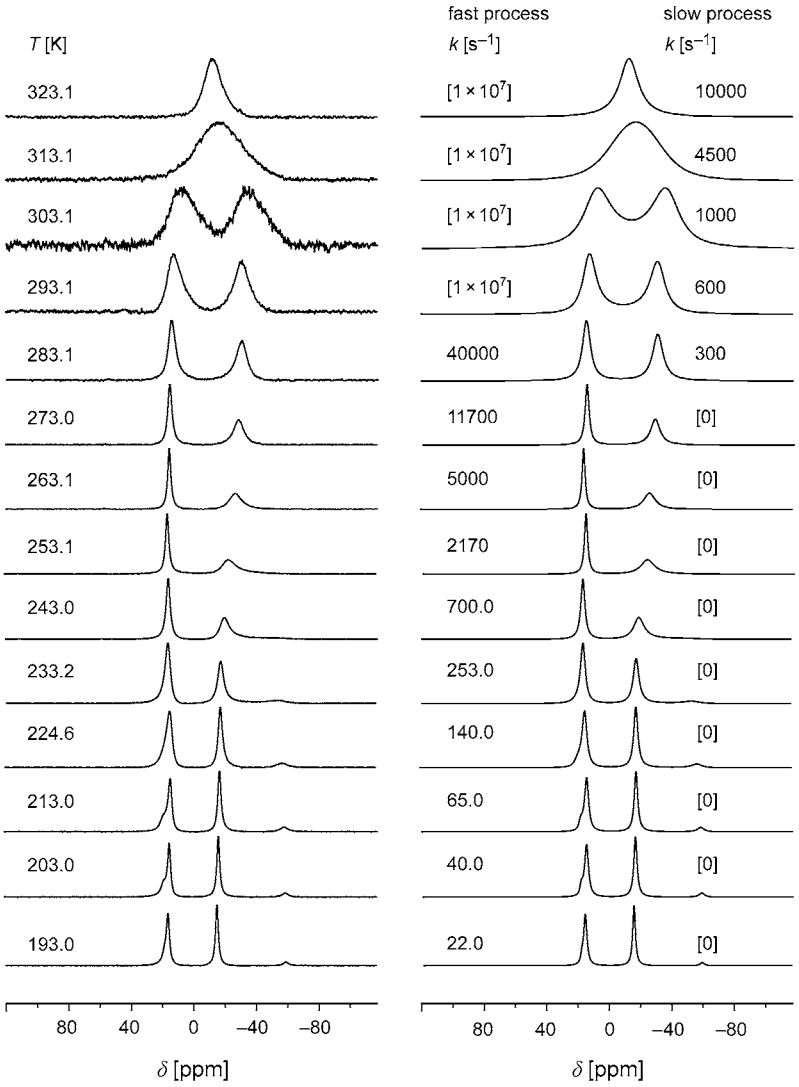

Fig. 6. *Experimental* (left) *and simulated* (right) *^{133}Cs{^{1}H}-NMR spectra of* **4** *in (D_6)acetone at different temperatures.* In the simulated spectra, negligible exchange rates for the slow process at low temperatures ('zero') and for the fast process at high temperatures ('extremely fast') are given in brackets. The relative concentrations of the involved species were obtained by integration of the signals observed separately at low temperatures and extrapolation beyond coalescence (see *Supporting Information*).

(δ 14.6 ppm at $-60°$). At $-20°$, coalescence occured between the weak signal at highest field (-58.6 ppm) and the intense signal (-16.9 ppm), while the two nearly isochronous signals at 14.6 ppm remained unaffected. Subesquently, between $+30°$ and $+40°$, coalescence was observed for the signals at 14.6 and -16.9 ppm, respectively.

These observations must be explained by two independent exchange processes which take place for **4** in (D_6)acetone solution. The corresponding *Eyring* plots for these processes are depicted in *Fig. 7*. From these data, the following kinetic parameters were extracted:

'Fast' process:

$$\Delta H^{\ddagger} = 11.7 \pm 0.5 \text{ kcal/mol}$$

$$\Delta S^{\ddagger} = +3.3 \pm 0.1 \text{ cal/(K mol)}$$

For the coalescence temperature of this process, $\Delta G^{\ddagger}_{253} = 10.8$ kcal/mol is computed.

'Slow' process:

$$\Delta H^{\ddagger} = 15.7 \pm 1.9 \text{ kcal/mol}$$

$$\Delta S^{\ddagger} = +8.0 \pm 0.9 \text{ cal/(K mol)}$$

For the coalescence temperature of this process, $\Delta G^{\ddagger}_{308} = 13.2$ kcal/mol is computed.

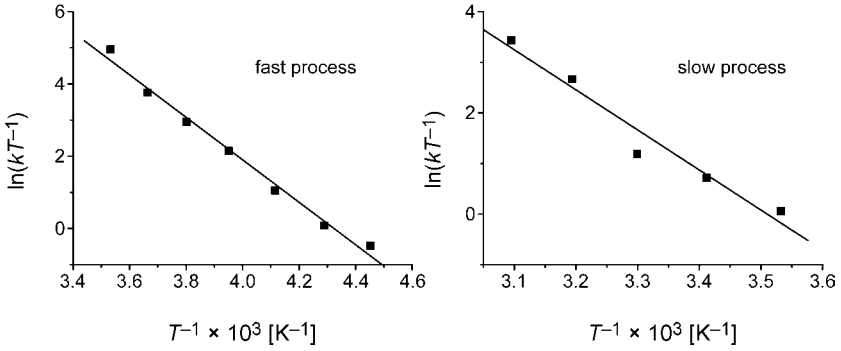

Fig. 7. Eyring *plots for the simulated data of* Fig. 6 *for the 'fast' and the 'slow' processes observed in* **4**

The spectra depicted in *Fig. 6* may also be analyzed by 'approximate methods'. By using the well-known *Gutowsky–Holm* equation [9], we obtain $\Delta G^{\ddagger}_{253} = 10.3$ kcal/mol (fast process) and $\Delta G^{\ddagger}_{308} = 12.9$ kcal/mol (slow process).

These data agree well with the 'more accurate' data from the complete line-shape analysis for **4**.

As a first interpretation of the dynamic phenomena observed in **4**, we speculated about an exchange between 'end-on' and 'side-on' Cs for the fast process and an '*endo*/*exo*' exchange for the slow process (*Scheme 3*).

It is well-known that alkali organometallic compounds may co-exist as an equilibrium of contact ion-pairs (CIP) and solvent-separated ion-pairs (SSIP) [10]. As early as 1966, *Hogen-Esch* and *Smid* [11] described separate observation of CIPs and SSIPs by using UV spectroscopy. Since UV is a fast method, also relatively rapid exchange processes permit separate observation of CIPs and SSIPs. By contrast, NMR as being a 'slow' method usually yields averaged signals for CIPs and SSIPs [12].

Scheme 3

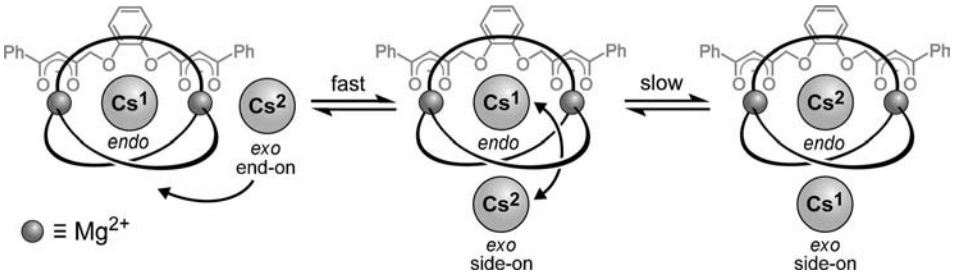

Separate observation of CIPs and SSIPs by NMR was possible only in rare cases, noteworthy, when HMPA is present as a ligand [13] or at very low temperatures for THF or Et_2O as ligands [14]. Here, we present a new example for separate CIP/SSIP observation by using ^{133}Cs-NMR.

Based on this CIP-SSIP interpretation, we abandoned our initial hypothesis outlined in *Scheme 3:* we still interpret the slow process for **4** as an *endo*-Cs/*exo*-Cs exchange. However, the rapid process must rather be attributed to ion-pair phenomena. Our current interpretation of the dynamic processes for **4** is presented in *Scheme 4*. Here, we assume the presence of an '*endo*'-Cs and an '*exo*'-Cs, the latter being located 'end-on' or 'side-on'. Presumably, this 'end-on'/'side-on' exchange is a very rapid process in solution on the NMR time scale, and only averaged signals are observed in the ^{133}Cs-NMR spectrum. However, we additionally suggest an ion-pair process which involves Cs tightly bound to the anion (the 'cage' which surrounds '*endo*' Cs), *i.e.*, a CIP (*Scheme 4*, *top*) and an '*exo*' Cs surrounded by solvent molecules (acetone), *i.e.*, an SSIP (*Scheme 4*, *bottom*). This CIP/SSIP exchange must be the 'fast' process observed in the ^{133}Cs-NMR spectra described above.

Scheme 4

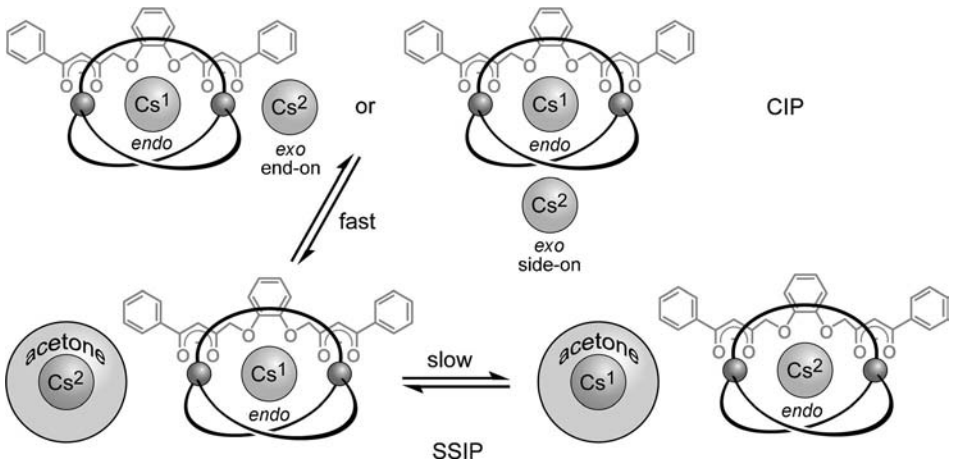

To confirm our hypothesis of a CIP/SSIP exchange for the rapid process observed for **4** in acetone, we prepared a solution of **4** in a *ca.* 1:1 mixture (D_6)acetone (for lock)/non-deuterated acetone (for heteronuclear ^1H,^{133}Cs NOE).

The heteronuclear nuclear *Overhauser* effect (NOE) is a well-known phenomenon that has been extensively exploited, also by one of the authors (*W. B.*) [15]. We have previously demonstrated that two-dimensional heteronuclear *Overhauser* spectroscopy (HOESY) [16] may be applied also to the isotope pairs ^1H,^{133}Cs [17]. Thus, close spatial relationships between these nuclei may be detected. In addition, 'inverse' measurements (by directly detecting ^1H rather than the heteronucleus) further enhances the sensitivity. These types of measurement may be conveniently carried out by the inclusion of pulsed-field gradients [18].

We have carried out an inverse pulsed-field gradient ^1H,^{133}Cs-HOESY experiment on **4** in (D_6)acetone/acetone at $-59°$ (*Fig. 8*).

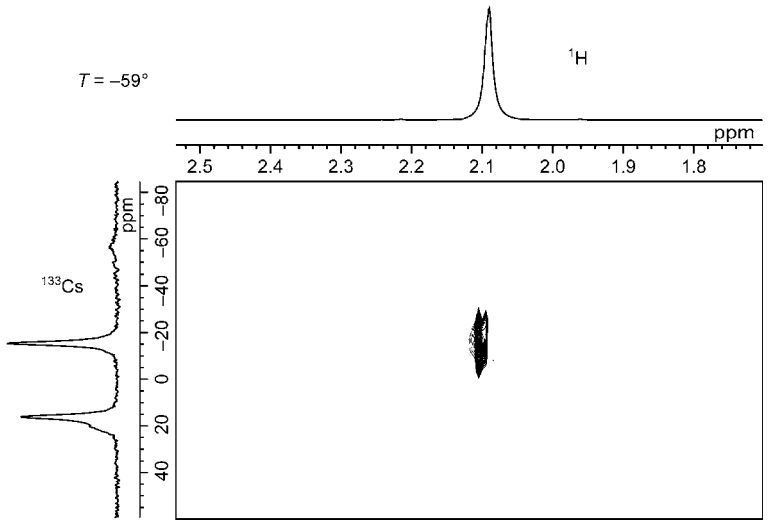

Fig. 8. *Pulsed field gradient inverse ^{133}Cs,^1H-HOESY spectrum of* **4** *in (D_6)acetone/acetone 1:1 at $-59°$; mixing time, 100 ms.* The cross-peak is assigned to the *exo* Cs ion, surrounded by solvent molecules (SSIP).

An intense cross-peak was detected which involves the ^1H-signal of non-deuterated acetone and the ^{133}Cs signal at -16.9 ppm. This indicates close proximity of this Cs species to the surrounding solvent molecules. No cross-peaks were detected for the Cs species which resonate at *ca.* 14.6 ppm. Thus, these Cs ions must be more remote to the acetone solvent molecules. We emphasize that we should also expect a cross-peak between the ^1H resonance of acetone and the weak ^{133}Cs signal at -58.6 ppm at a very good signal-to-noise ratio. This is due, on the one hand, to presumed peripheral solvation also of a CIP by acetone. On the other hand, at the recording temperature of $-59°$ in *Fig. 8*, there is already appreciable exchange between the CIP and the SSIP. Thus, a transferred heteronuclear NOE should be expected [19]. However, under the recording conditions of *Fig. 8*, the signal-to-noise ratio is too small for this cross-peak detection.

As a further corroboration for our assumptions on the ion-pair phenomena, we carried out a simple ^{133}Cs-NMR experiment (*Fig. 9*).

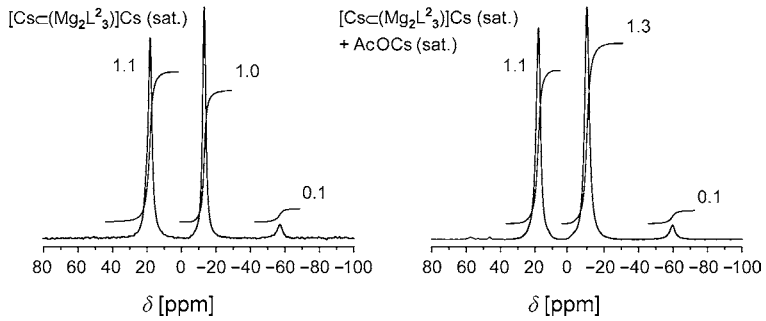

Fig. 9. *^{133}Cs{^{1}H}-NMR Spectrum of* **4** *in (D_6)acetone at* $-80°$ (saturated solution) *with integrals and integral heights. Left:* without added AcOCs; *right:* with added AcOCs (saturated). Note the intensity increase of the signal at *ca.* -10 ppm, thus assigning the *exo* Cs ion involved in the SSIP.

Here, the spectrum on the left side shows the ^{133}Cs-NMR spectrum of **4** in (D_6)acetone at $-80°$, *i.e.*, under conditions of slow exchange even for the 'rapid' CIP/SSIP process. The integral numbers must be interpreted as follows: the signal at 18.0 ppm is the overlayed signal of '*endo*'-Cs both of the CIP and the SSIP. The signal at -10.1 ppm (normalized to 1.00) corresponds to the '*exo*'-Cs of the SSIP, and the weak signal at -59.9 ppm to the '*exo*'-Cs of the CIP. When AcOCs is added to the solution (*Fig. 9*, right), the only intensity increase is observed for the signal at -10.1 ppm. Thus, this must be a common signal of '*exo*'-Cs in the SSIP of **4** and Cs from AcOCs, likewise present as being solvated by solvent molecules.

The mutual exchange processes for **4** may also be demonstrated by ^{133}Cs-EXSY spectra [20] (*Fig. 10*).

A ^{133}Cs-EXSY spectrum recorded at $-70°$ (*Fig. 10*, top) revealed a pair of cross-peaks between the signal at -16.1 ppm (assigned to '*exo*'-Cs of the SSIP) and that at -58.9 ppm (assigned to '*exo*' Cs of the CIP). Inherently, the cross-peak at δ -58.9 ppm in f_2 and δ -16.1 ppm in f_1 was much less intense than the corresponding one, reflecting the different populations of the involved species.

A second ^{133}Cs-EXSY spectrum has been recorded at 0°, *i.e.*, under conditions where the rapid CIP/SSIP process is already far above coalescence (*Fig. 10*, bottom). Here, we observed a pair of cross-peaks of equal intensity for '*endo*'-Cs at δ 14.4 ppm and '*exo*'-Cs at δ -29.9 ppm. This indicates the mutual exchange of these Cs sites at this temperature.

To confirm the monomeric nature of **4** in acetone solution rather than the polymeric shape observed in the crystal, we carried out ^{1}H-DOSY [21] recordings (not depicted). Diffusion-ordered spectroscopy ('DOSY') is an NMR tool for determining molecule sizes. From these data, obtained at $+30°$, a hydrodynamic radius of 5.40×10^{-9} m for **4** was obtained. As an arbitrary internal reference, the hydrodynamic radius of acetone, obtained from the same recordings, of 1.97×10^{-9} m has been employed. This clearly indicates that **4** must be a monomeric entity in acetone solution.

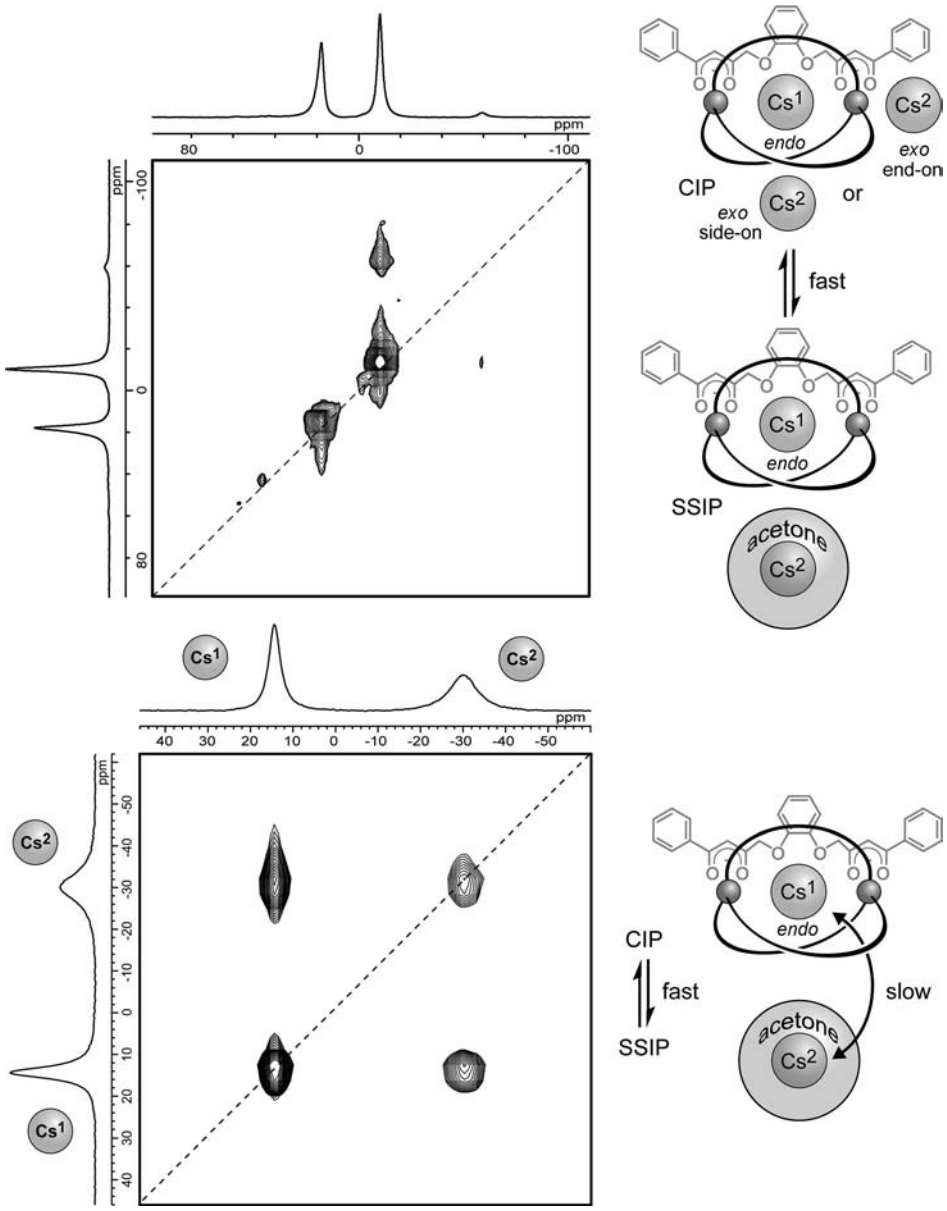

Fig. 10. *^{133}Cs{^{1}H}-EXSY NMR Spectra of* **4** *in (D_6)acetone. Top:* at $-70°$; mixing time, 10 ms, indicating the fast process (CIP/SSIP exchange of the *exo*-Cs ions); *bottom:* at 0°; mixing time, 10 ms, indicating the slow process (exchange of *endo*- and *exo*-Cs ions).

Methyl Complex **2**. The ^{1}H- and ^{13}C-NMR spectra of **2** have been previously described, along with an X-ray structural analysis [1]. In contrast to the solid-state structure of **4** (meandering; *cf. Scheme 2*), a linear polymeric arrangement of '*endo*'-Cs

(surrounded by three ligands) and '*exo*'-Cs was found (see *Scheme 1*). Accordingly, a solid-state ^{133}Cs-NMR spectrum of **2** revealed only two signals (*Fig. 11*), assigned to '*endo*'-Cs at δ 70.0 ppm and '*exo*'-Cs at δ −60.8 ppm.

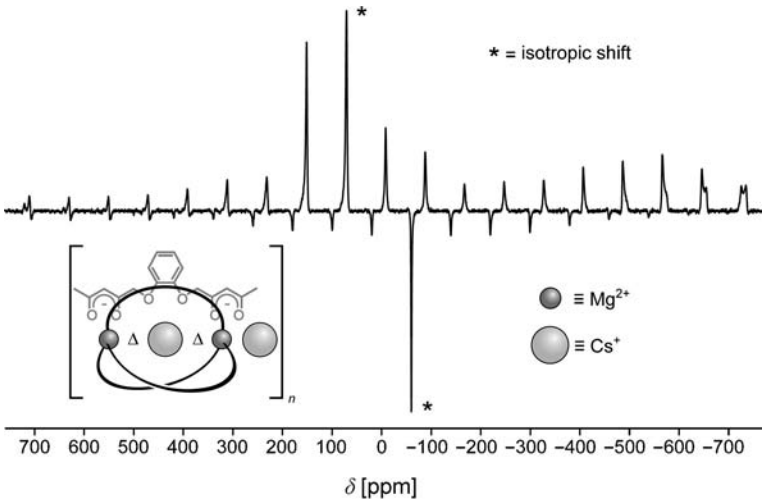

Fig. 11. *Solid-state ^{133}Cs{^{1}H}-MAS-NMR spectrum of* **2**, *recorded in the 'inversion recovery' mode* (180° – delay – 90° – FID). Delay time between pulses: 1.2 s, chosen such that the faster-relaxing *endo*-Cs signal points upward and the slower-relaxing *exo*-Cs signal points downward. Isotropic shifts are marked by an asterisk, other signals are spinning side bands. Spinning speed, 6034 Hz.

The spectrum shown in *Fig. 11* has been recorded in the 'inversion recovery' mode. The delay between the 180° pulse and the 90° pulse was chosen such that the faster-relaxing '*endo*'-Cs signal points upward and the slower-relaxing '*exo*'-Cs signal points downward. Note the larger chemical-shift anisotropy (CSA) of the '*endo*'-Cs as compared to the '*exo*'-Cs, indicated by the larger 'spreading' of spinning side bands for the former species.

Solution ^{1}H- and ^{13}C-NMR spectra exhibited sharp signals for **2**, similar to phenyl complex **4**. Hence, we concluded that we were dealing with similar situations as described above for **4**. At present, we suggest that similar CIP/SSIP phenomena should be found for **2**. The ^{13}C-NMR spectrum of **2**, by close inspection with strong resolution enhancement (*Gauss* window), exhibits the same signal splitting as described above for **4**, *i.e.*, a double set of signals. As for **4**, we interpret this phenomenon as the presence of a racemate ($\Delta,\Delta;\Lambda,\Lambda$) and a *meso*-species ($\Delta,\Lambda$) under slow exchange on the NMR time-scale at room temperature [6].

Unfortunately, the solubility of **2** in acetone is considerably lower as compared to phenyl complex **4**. Thus, especially at lower temperatures, detailed NMR studies as described above for **4** are precluded for **2**. However, we assume that the effects observed for **4** (exchange phenomena, ion-pair effects) must be similar.

Conclusions. – We have described the new X-ray structure of self-complementary {2}-metallocryptate **4**. Similar to the previously described solid-state structures of the analogous $[Cs\subset\{Co_2(L^2)_3\}]Cs$ and $[Rb\subset\{Mg_2(L^2)_3\}]Rb$ complexes, a meandering

structure of Cs ions was found. Herein, '*endo*'-Cs (surrounded by three organic ligands **3**) is counter-balanced by alternating 'end-on' and 'side-on' Cs ions. The solid-state ^{133}Cs-NMR spectrum nicely confirmed these findings: there are four different Cs sites being observed. By contrast, monomeric entities of **4** are present in solution. There exist interesting dynamic phenomena which must be attributed to ion-pair phenomena: in acetone solution, contact ion pairs (CIP) co-exist along with solvent-separated ion-pairs (SSIP), with slow exchange on the NMR time-scale at low temperatures. Kinetic parameters of two different dynamic processes have been determined, *i.e.*, the exchange of the '*exo*'-Cs between CIP and SSIP, and the exchange of 'inner' (*endo*) and 'outer' (*exo*) Cs. Various NMR experiments (EXSY, addition of AcOCs, DOSY, full line-shape analysis) have helped to confirm the underlying assumptions.

Methyl complex **2** has been likewise studied by ^{133}Cs solid-state NMR. The linear polymer structure found previously by X-ray has been confirmed, as only two signals were detected.

The results described in this article highlight the importance of solid-state NMR spectroscopy. In particular, ^{133}Cs solid-state NMR spectra provide valuable insights into these structures and are in full agreement with the structures found by X-ray analysis. Thus, solid-state ^{133}Cs-NMR corroborates its role as a 'link' between X-ray and solution NMR. Moreover, solution-state ^{133}Cs-NMR turned out to be a valuable tool for the study of dynamic processes. Despite its spin quantum number of $I = 7/2$, ^{133}Cs may be employed and treated in many respects in the same way as the 'good' spin-1/2 nuclei ^{1}H and ^{13}C, even in heteronuclear NOE experiments.

Experimental Part

{2}-Metallocryptates **2** and **4** where synthesized as described in [1].

X-Ray Crystal-Structure Analysis. Crystals of *meso*-(**4**)$_n$ suitable for X-ray-analysis were obtained by vapor diffusion of Et_2O into the filtrate of the crude reaction mixture as colorless blocks. Intensity data were collected on a *Bruker Smart APEX 2* diffractometer using graphite monochromatized MoK_α radiation ($\lambda = 0.71073$ Å). Data were corrected for *Lorentz* and polarization effects; a semi-empirical absorption correction on the basis of multiple scans was applied (SADABS 2008/1) [22]. The structure was solved by direct methods, and refinement was carried out by full-matrix least-squares procedures on F^2 with SHELXTL NT 6.12 (*Bruker AXS*, 2002) [23]. All non-H-atoms were refined anisotropically. The compound crystallized as solvate with a total of 2.24 Et_2O and 2.26 MeCN molecules in the asymmetric unit. These solvent molecules were partially disordered and shared in part common crystallographic sites. Two of the Ph rings of the ligands were disordered. Two alternative orientations were refined resulting in site occupancies of 50.9(4) and 49.1(4)% for C(15) – C(20) and C(15A) – C(20A), and of 69.7(4) and 30.3(4)% for C(41) – C(46) and C(41A) – C(46A), resp. (for numbering, see *Supporting Information*). SIMU, ISOR, and SAME restraints were applied in the refinement of the disordered structure parts. All H-atoms were placed in positions of optimized geometry, their isotropic displacement parameters were tied to those of their corresponding carrier atoms by a factor of 1.2 or 1.5. Molecular graphics were designed by using PLATON [24], MOLMOL, and POV-Ray. The crystal data and details concerning data collection and structural refinement are given in the *Table*. CCDC-895436 contains the supplementary crystallographic data for this article. These data can be obtained free of charge *via* http://www.ccdc.cam.ac.uk/data_request/cif.

NMR Spectroscopy. NMR Spectra (^{1}H, ^{13}C, ^{133}Cs) were recorded on a *JEOL Alpha500* spectrometer (11.7 T, ^{1}H, 500 MHz). Solid-state MAS spectra were recorded by using a 6-mm rotor with spinning speeds of 6117 Hz for **4** (*Fig. 3*) and 6034 Hz for **2** (*Fig. 11*). Solution spectra were recorded on a multinuclear 5-mm probehead and an inverse 5-mm probehead with actively shielded gradient coils, resp.

Table. *Crystallographic Data of Compound* meso-(**4**)$_n$

Empirical formula	$C_{173.5}H_{155.22}Cs_4Mg_4N_{4.27}O_{38.24}$
M_r	3540.82
Crystal size [mm]	$0.38 \times 0.24 \times 0.12$
Unit cell parameters:	
a [Å]	25.5967(4)
b [Å]	21.7216(4)
c [Å]	29.8491(5)
β [°]	91.122(1)
V [Å^3]	16593.0(5)
Crystal system	monoclinic
Space group	$P2_1/n$
Z	4
D_x [g cm^{-3}]	1.417
μ [mm^{-1}]	0.964
T_{min}; T_{max}	0.652; 0.746
Number of reflections (N): collected	206013
unique	34363
observed ($F_o \geq 4.0\sigma(F)$):	23834
Number of reflections used for cell refinement	9778
Range (°)	$4.8 \leq 2\Theta \leq 52.3$
Number of refined parameters (p)	2175
$\Delta\rho$ (max./min.) [e Å^{-3}]	1.533; −1.289
Final R indices	$R_1 = 0.0458$; $wR_2 = 0.1291$ [a])
Goodness-of-fit on F^2	1.264

[a]) Weighting scheme: $w = 1/[\sigma^2(F_o^2) + (0.0540\,P)^2 + 3.2945\,P$ where $P = (F_o^2) + 2F_c^2)/3$

Chemical shifts (δ, [ppm]) are referenced to $CDCl_3$ (residual signal, 7.24 ppm, ^{1}H; 77.0 ppm, ^{13}C), (D_6)acetone (residual signal, 2.04 ppm, ^{1}H; 29.8 ppm, ^{13}C), (D_6)DMSO (residual signal, 2.49 ppm, ^{1}H; 39.5 ppm, ^{13}C), CD_3OD (residual signal, 3.30 ppm, ^{1}H; 49.0 ppm, ^{13}C), and $CsNO_3$ (0.0 ppm, ^{133}Cs, 1M soln. in D_2O for soln. spectra, 0.0 ppm powdered crystals for solid-state spectra). Coupling constants J are given in Hz.

Inverse (^{1}H-detected) ^{1}H,^{133}Cs-pulsed field gradient HOESY spectrum of **4** in (D_6)acetone/acetone 1:1 (*Fig. 8*): 2k data points in f_2, spectral width in f_2 5327 Hz, 128 scans per t_1-increment, acquisition time 0.38 s, relaxation delay 3.0 s, spectral width in f_1 9451 Hz, 16 t_1-increments, zero-filled to 32; mixing time, 100 ms; trapezoidal window in t_2, exponential window (BF 50) in t_1; temp., −59°. Due to the manufacturer's hardware limit, no temp. lower than −59° are permitted at this employed probehead.

^{133}Cs{^{1}H}-EXSY Spectrum of **4** (*Fig. 6*, *top* and *bottom*): mixing time, 10 ms; spectral width in f_1 and f_2, 15649 Hz; 256 data points in f_2; acqusition time, 16.4 ms; relaxation delay, 86 ms; 64 t_1-increments, 1024 scans per t_1-increment; phase-sensitive, exponential window in t_2, Gaussian window in t_1; measuring time, 1.5 h.

^{1}H-DOSY Recordings of **4** in (D_6)acetone were carried out by using the inverse field-gradient probehead at +30°. The BPP-STE-LED[3]) sequence has been employed. A total of 32 increasing gradient strengths were applied with a constant diffusion delay of 50 ms. Maximum gradient strength: 42.5 G/cm. The calculated hydrodynamic radius is an average of the numbers obtained for the proton signals of **4**. The internal reference for the calculation of the hydrodynamic radius of **4** is the solvent signal (acetone, $r_H = 1.97 \times 10^{-9}$ m) [25]. The built-in procedure for T_2 measurements of the spectrometer

[3]) BPP-STE-LED = Bipolar pulse stimulated echo longitudinal encoding decoding; for pulse sequence, see [21].

software has been used for the calculations (plot of $\ln(I/I_0)$ *vs.* G^2, evaluation of the slope of the linear regression curve) in order to obtain a 'pseudo-DOSY' evaluation.

$^{133}Cs\{^1H\}$ Solid-state MAS NMR spectrum of **2** (*Fig. 11*): inversion recovery method, spectral width, 100 kHz; 2-k data points, zero filled to 8 k; acquisition time, 20 ms; relaxation delay, 10 s; delay between 180° and 90° pulse, 1.2 s; 4542 scans; spinning speed, 6034 Hz; measuring time, 1.5 h.

Simulations of the ^{133}Cs NMR spectra (*Fig. 6*) were carried out by using the 'gNMR' software package by *P. Budzelaar*[4]), Version 5.01.

The authors gratefully acknowledge financial support by the *Deutsche Forschungsgemeinschaft* (*DFG*), Projects BA 809/2-1 and SA 276/29-1. The generous allocation of X-ray facilities by Professor *K. Meyer*, Lehrstuhl für Anorganische and Allgemeine Chemie, Universität Erlangen-Nürnberg, is gratefully acknowledged.

REFERENCES

[1] R. W. Saalfrank, N. Mooren, A. Scheurer, H. Maid, F. W. Heinemann, F. Hampel, W. Bauer, *Eur. J. Inorg. Chem.* **2007**, 4815; R. W. Saalfrank, H. Maid, A. Scheurer, *Angew. Chem.* **2008**, *120*, 8924; *Angew. Chem., Int. Ed.* **2008**, *47*, 8794; R. W. Saalfrank, A. Scheurer, *Top. Curr. Chem.* **2012**, *319*, 125.
[2] R. M. Izatt, K. Pawlak, J. S. Bradshaw, R. L. Bruening, *Chem. Rev.* **1995**, *95*, 2529.
[3] E. Mei, A. I. Popov, J. L. Dye, *J. Am. Chem. Soc.* **1977**, *99*, 6532; E. Mei, L. Liu. J. L. Dye, A. I. Popov, *J. Solution Chem.* **1977**, *6*, 771; E. Kauffmann, J. L. Dye, J. M. Lehn, A. I. Popov, *J. Am. Chem. Soc.* **1980**, *102*, 2274.
[4] S. Burk, M. Albrecht, K. Hiratani, *J. Incl. Phenom. Macrocycl. Chem.* **2008**, *61*, 353.
[5] R. W. Saalfrank, H. Maid, N. Mooren, F. Hampel, *Angew. Chem.* **2002**, *114*, 323; *Angew. Chem., Int. Ed.* **2002**, *41*, 304.
[6] M. Albrecht, *Chem. – Eur. J.* **2000**, *6*, *3485*; J. Xu, T. N. Parac, K. N. Raymond, *Angew. Chem.* **1999**, *111*, 3055; *Angew. Chem., Int. Ed.* **1999**, *38*, 2878.
[7] R. W. Saalfrank, H. Maid, A. Scheurer, R. Puchta, W. Bauer, *Eur. J. Inorg. Chem.* **2010**, 2903; R. W. Saalfrank, B. Demleitner, H. Glaser, H. Maid, D. Bathelt, F. Hampel, W. Bauer, M. Teichert, *Chem. – Eur. J.* **2002**, *8*, 2679.
[8] I. Janser, M. Albrecht, K. Hunger, S. Burk, K. Rissanen, *Eur. J. Inorg. Chem.* **2006**, 244.
[9] H. S. Gutowsky, C. H. Holm, *J. Chem. Phys.* **1956**, *25*, 1228; J. Sandström, 'Dynamic NMR Spectroscopy', Academic Press, London 1982, p. 79f.
[10] S. Winstein, E. Clippinger, A. H. Fainberg, G. C. Robinson, *J. Am. Chem. Soc.* **1954**, *76*, 2597.
[11] T. E. Hogen-Esch, J. Smid, *J. Am. Chem. Soc.* **1966**, *88*, 307.
[12] D. Hoffmann, W. Bauer, P. v. R. Schleyer, *J. Chem. Soc., Chem. Commun.* **1990**, 208.
[13] H. J. Reich, R. R. Dykstra, *Angew. Chem.* **1993**, *105*, 1489; *Angew. Chem., Int. Ed.* **1993**, *32*, 1469.
[14] B. L. Lucht, D. B. Collum, *J. Am. Chem. Soc.* **1994**, *116*, 6009.
[15] J. Betz, W. Bauer, *J. Am. Chem. Soc.* **2002**, *124*, 8699; W. Bauer, in 'Lithium Chemistry: A Theoretical and Experimental Overview', Eds. A.-M. Sapse, P. v. R. Schleyer, John Wiley & Sons, New York, 1995, p. 125f.; W. Bauer, P. v. R. Schleyer, in 'Recent Results in NMR Spectroscopy of Organolithium Compounds', Ed. V. Snieckus, 'Advances in Carbanion Chemistry', Jai Press, Greenwich (Connecticut), 1992, Vol. 1, 89; D. Hoffmann, W. Bauer, P. v. R. Schleyer, *J. Chem. Soc., Chem. Comm.* **1990**, 208; W. Bauer, P. v. R. Schleyer, *Magn. Reson. Chem.* **1988**, *26*, 827.
[16] C. Yu, G. C. Levy, *J. Am. Chem. Soc.* **1984**, *106*, 6533.
[17] W. Bauer, *Magn. Reson. Chem.* **1991**, *29*, 494.
[18] W. Bauer, *Magn. Reson. Chem.* **1996**, *34*, 532.
[19] D. Neuhaus, M. P. Williamson, 'The Nuclear Overhauser Effect in Structural and Conformational Analysis', 2nd edn., Wiley-VCH, New York, 2000, p. 178f.

---

4) *gNMR* Spin simulation software by *Peter H. M. Budzelaar*, University of Manitoba, Winnipeg (Canada), distributed commercially by *Adept Scientific* until 2005, is now available free: URL http://home.cc.umanitoba.ca/~budzelaa/gNMR/gNMR.html.

[20] U. C. Meier, C. Detellier, *J. Phys. Chem. A* **1998**, *102*, 1888.
[21] B. Antalek, *Concepts Magn. Reson.* **2002**, *14*, 225; C. S. Johnson Jr., *Prog. NMR Spectrosc.* **1999**, *34*, 203; W. S. Price, *Concepts Magn. Reson.* **1997**, *9*, 299; W. S. Price, *Concepts Magn. Reson.* **1998**, *10*, 197; P. Stilbs, *Progr. NMR Spectrosc.* **1987**, *19*, 1.
[22] *SADABS*, *Bruker AXS, Inc.*, 2009, Madison WI, USA.
[23] G. M. Sheldrick, *Acta Crystallogr., Sect. A* **2008**, *64*, 112.
[24] A. L. Spek, *Acta Crystallogr.*, *Sect. D* **2009**, *65*, 148.
[25] S. Viel, F. Ziarelli, G. Pagès, C. Carrara, S. Caldarelli, *J. Magn. Reson.* **2008**, *190*, 113.

Received August 24, 2012